Chinese Chemical Letters 34 (2023) 107621

Contents lists available at ScienceDirect

Chinese Chemical Letters

journal homepage: www.elsevier.com/locate/cclet

Recent advances in H_2O_2-based advanced oxidation processes for removal of antibiotics from wastewater

Xuechun Wang[a,b,c], Jiana Jing[a,b,c], Minghua Zhou[a,b,c,*], Raf Dewil[d]

[a] Key Laboratory of Pollution Process and Environmental Criteria, Ministry of Education, College of Environmental Science and Engineering, Nankai University, Tianjin 300350, China
[b] Tianjin Key Laboratory of Environmental Technology for Complex Trans-Media Pollution, Nankai University, Tianjin 300350, China
[c] Tianjin Advanced Water Treatment Technology International Joint Research Center, College of Environmental Science and Engineering, Nankai University, Tianjin 300350, China
[d] Department of Chemical Engineering, KU Leuven, J. De Nayerlaan 5, Sint-Katelijne-Waver B-2860, Belgium

ARTICLE INFO

Article history:
Received 15 March 2022
Revised 6 June 2022
Accepted 17 June 2022
Available online 22 June 2022

Keywords:
Advanced oxidation processes
H_2O_2 *in-situ* generation
Antibiotics degradation
Combined AOPs
Wastewater treatment

ABSTRACT

As important emerging contaminants, antibiotics have caused potential hazards to the ecological environment and human health due to their extensive production and consumption. Among various techniques for removing antibiotics from wastewater, H_2O_2-based advanced oxidation processes (AOPs) have received increasing attention due to their fast reaction rate and strong oxidation capability. Hence this review critically discusses: (i) Recent research progress of AOPs with the addition of H_2O_2 for antibiotics removal through different methods of H_2O_2 activation; (ii) recent advances in AOPs that can *in-situ* generate and activate H_2O_2 for antibiotics removal; (iii) H_2O_2-based AOPs as a combination with other techniques for the degradation and mineralization of antibiotics in wastewater. Future perspectives about H_2O_2-based AOPs are also presented to grasp the future research trend in the area.

1. Introduction

In recent years, the presence of antibiotics in natural water bodies has gained extensive attention from the environmental protection community, as they cause great harm to water bodies and the natural environment, even when present in trace concentration. Discharged mainly from pharmaceutical industries, hospitals, and the use of veterinary drugs in animal husbandry and aquaculture [1,2], antibiotic residuals have been frequently detected in various water bodies worldwide including rivers, lakes, sea water and even drinking water [3]. Their presence poses serious risks to the environment and human health since they increase antibiotic-resistance of microbial communities and cause non-negligible alterations in food chains [4].

To substantially remove antibiotics from water, various treatment processes have been explored, including coagulation, membrane separation, adsorption, biodegradation and advanced oxidation processes (AOPs). AOPs are emerging and prominent methods and have attracted wide attention due to their excellent oxidation capacity and high practical applicability [5,6]. AOPs based on hydrogen peroxide (H_2O_2), being a versatile, eco-friendly, and strong oxidizing chemicals, have received great acceptance due to their high degradation efficiency and environmental compatibility [7]. Thus, extensive research has been focused on these H_2O_2-based AOPs and their combination with other techniques for antibiotics removal from wastewater [8].

Some review papers on the AOPs for the treatment of antibiotics in wastewater have been published in recent years [9–13], the fundamental mechanism of various conventional and emerging technologies for removal of antibiotics has been summarized. For example, Wang and Zhuan [11] summarized the recent advance in antibiotics degradation by AOPs such as Fenton reaction, ozonation or catalytic ozonation, photocatalytic oxidation, electrochemical oxidation, and ionizing radiation, and discussed several important influencing factors and the applications for antibiotics removal in water and wastewater. Alexsandro [12] reviewed the development of electrochemical AOPs for the treatment of antibiotics present in synthetic and real wastewaters, and discussed their fundamentals. However, no comprehensive review is available that summarizes the current research status of the *in-situ* or *ex-situ* H_2O_2 and further applications in AOP for antibiotics removal from wastewater.

---

* Corresponding author at: Key Laboratory of Pollution Process and Environmental Criteria, Ministry of Education, College of Environmental Science and Engineering, Nankai University, Tianjin 300350, China.

E-mail address: zhoumh@nankai.edu.cn (M. Zhou).

https://doi.org/10.1016/j.cclet.2022.06.044

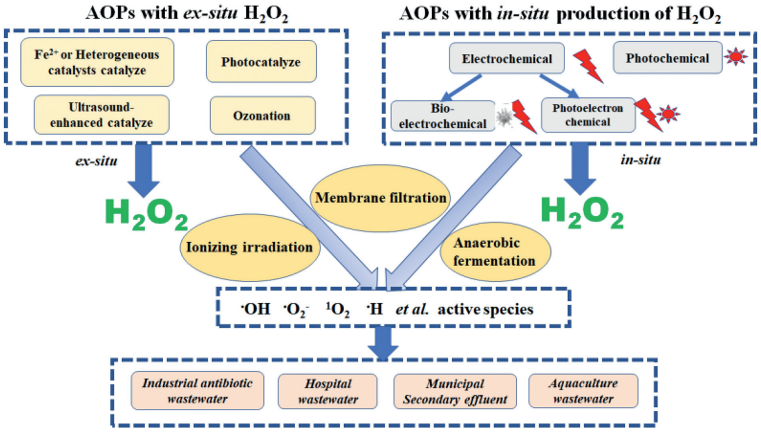

Fig. 1. H_2O_2 based AOP for removal of antibiotics in water and secondary wastewater.

Therefore, this review will focus on the major advances in *in-situ* or *ex-situ* H_2O_2-based AOPs for removal of antibiotics from wastewater effluents. As depicted in Fig. 1, this review systemically summarizes recent AOP studies with added H_2O_2 or *in-situ* produced H_2O_2 through electrochemical, photochemical, bio-electrochemical and photo-electrochemical methods. Furthermore, H_2O_2-based AOPs combined with other techniques (*e.g.*, membrane filtration, anaerobic fermentation) for the degradation of antibiotics from various wastewaters are discussed. In addition, the prospects and challenges for the development of H_2O_2-based AOPs are suggested.

2. AOPs with *ex-situ* H_2O_2

2.1. Fenton process

The classical Fenton process is widely used in wastewater treatment. In this process, Fenton reagents (Fe^{2+} and H_2O_2) are added and react with each other to form hydroxyl radicals ($^{\bullet}OH$) to degrade various pollutants, following the simplified reaction shown in Eq. 1 [14].

$$Fe^{2+} + H_2O_2 \rightarrow Fe^{3+} + {}^{\bullet}OH + OH^- \quad (1)$$

Advantages of Fenton oxidation are the high degradation efficiency and easy operation, however, it also has several drawbacks such as the generation of (large amounts of) iron sludge, and its narrow and highly acidic optimal pH range (2–3) [15], which limit its application in wastewater treatment. To overcome these drawbacks, Fenton-like processes using different heterogeneous catalysts to replace Fe^{2+} have been developed rapidly in recent years [16–18]. Many kinds of iron-based materials, such as zero-valent iron (ZVI, Fe^0) [19,20], goethite (α-FeOOH) [21], hematite (α-Fe_2O_3) [22] and magnetite (Fe_3O_4) [23] have been used as heterogeneous Fenton catalysts. However, these catalysts generally result in a lower reaction rate for degrading pollutants than the classical Fenton [24].

Therefore, to solve this problem, there has been a shift in focus to the modification of heterogeneous Fenton catalysts and addition of external energy [25,26]. For example, pre-magnetization can increase the Fe^0 corrosion rate to generate Fe^{2+} owing to the "magnetic memory", which thus enhances the Fenton performance [26–28]. Moreover, to overcome the drawbacks of a narrow working pH range, chelating agents can chelate with Fe-ions, thus preventing their precipitation at neutral pH conditions, promoting Fenton or Fenton-like performance [29,30]. Ethylenediaminetetraacetic acid (EDTA) is one of the low-cost "green" chelating agents that has been widely applied [31–33]. As depicted in Fig. 2a, EDTA could complex Fe^{2+} to form the Fe^{2+}-EDTA complex, which catalyzes H_2O_2 faster to generate $^{\bullet}OH$ for sulfamethazine (SMT) removal. Pan *et al.* [34] found that only 19.4% SMT was removed by pre-Fe^0/H_2O_2 within 60 min at neutral pH, while 90.6% SMT was removed after the addition of 0.1 mmol/L EDTA. Meanwhile, the rate constant for SMT removal by pre-Fe^0-EDTA/H_2O_2 was 1.3 folds larger than that by Fe^0-EDTA/H_2O_2.

In addition to a single catalyst, the combination of various catalysts such as α-Fe_2O_3/TiO_2 [35], Fe^0/Fe_3O_4 [36], Fe^0/CeO_2 [37] and Si–Al/α-FeOOH [38] has been investigated to enhance the removal efficiency and the catalyst stability. Among them, carbon and iron composite catalysts have been widely used as heterogeneous Fenton catalysts for H_2O_2 activation due to their strong adsorption performance, mild reaction conditions, and limited by-products [39,40]. As shown in Fig. 2b, Zhou *et al.* [41] performed a comprehensive study to investigate H_2O_2 activation on a composite material comprising powder activated carbon (PAC) and ferroferric oxide nanocatalyst (C@FONC). Among them, PAC provides more adsorption active sites for the catalytic reaction, and FONC reacts with H_2O_2 to generate active radicals and accelerate the iron cycle. Tetracycline (TC) removal efficiency by the C@FONC/H_2O_2 system reached 97% within 120 min ($TC_0 = 150$ mg/L), which can be ascribed to the simultaneous occurrence of adsorption, Fenton-like reactions, and reduction reactions.

Meanwhile, several recent studies have shown that a fast electron transfer can be achieved through the strong combination of π-π and π-Fe interactions between the iron-carbon composite catalyst and antibiotics [42–44]. A novel strategy of constructing dual-reaction centers in a Fenton-like catalyst with a non-uniform distribution of electrons by a lattice doping method is shown in Fig. 2c. TC strongly interacts with graphene through π-π interactions and acts as an electron donor to transfer the electrons in TC *via* graphene to the iron species through π–Fe interactions to accelerate the conversion of Fe^{3+} to Fe^{2+}. The dual-reaction centers and the accelerated electron transfer thus promoted the $^{\bullet}OH$ production to achieve a higher TC (~15%) and TOC (~20%) removal with a lower iron leakage.

Bimetallic oxides (such as Fe-Cu, Fe-Co and Fe-Ce) also have been widely studied in recent years, showing promises in pollutants decomposition due to their great catalytic performance and superior electron transport capacities [45,46]. As shown in Fig. 2d, both Fe^{2+} and Co^{2+} react with H_2O_2 to form $^{\bullet}OH$, while Fe^{3+} and Co^{3+} react with H_2O_2 to form $^{\bullet}OH$ according to the Fenton mechanism. Meanwhile, the reaction of Fe^{2+} and Co^{3+} as depicted in Eq. 2 is thermodynamically favored. As such, Fe^{2+} and Co^{3+} can be continuously provided for H_2O_2 activation, generating more free radicals, thereby reaching significant removal of TC (83.5%) under

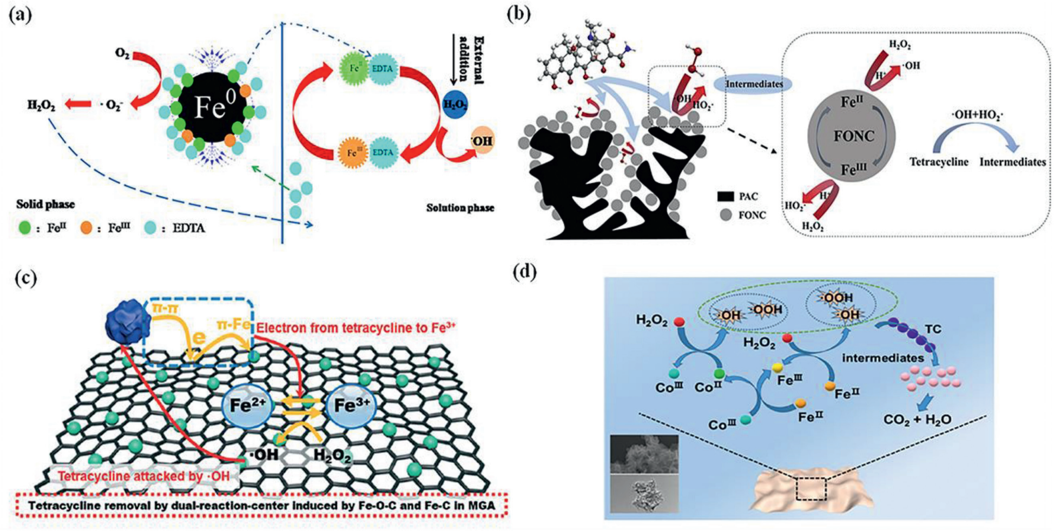

Fig. 2. (a) Reaction mechanisms for SMT removal by pre-Fe^0-EDTA H_2O_2 system. Copied with permission [34]. Copyright 2020, Elsevier. (b) Schematic diagram of the reaction mechanisms of TC degradation in the C@FONC/ H_2O_2 system. Copied with permission [41]. Copyright 2020, Elsevier. (c) Mechanism of antibiotic removal through a Fenton-like reaction by the Fe_3O_4@Fe/graphene aerogel. Copied with permission [48]. Copyright 2021, Elsevier. (d) Proposed mechanism of heterogeneous Fenton-like degradation of TC with CoFe-ONSs. Copied with permission [47]. Copyright 2021, Elsevier.

the neutral conditions after 50 min [47].

$$Co^{3+} + Fe^{2+} \rightarrow Co^{2+} + Fe^{3+} \quad (2)$$

2.2. Photocatalytic process with ex-situ H_2O_2

In the present research, the UV/H_2O_2 process has been increasingly used for degrading antibiotics in water and wastewater [49–53]. UV irradiation can degrade antibiotics *via* direct photolysis and $^{\bullet}OH$ produced by the decomposition of H_2O_2 through Eq. 3:

$$H_2O_2 + h\gamma \rightarrow 2\,^{\bullet}OH \quad (3)$$

It is acknowledged that the oxidation mechanism of UV/H_2O_2 includes two aspects: (1) The direct UV induced photolysis to destruct the chemical bonds and subsequent breakdown of the contaminant if it can absorb the UV light [54], (2) $^{\bullet}OH$ radical oxidation because of UV light absorption by H_2O_2 (the quantum yield for the process is 1 mol $^{\bullet}OH$ per Einstein absorbed by H_2O_2) [55].

In order to improve the degradation efficiency and mineralization rate of various refractory antibiotics, increasingly, researchers have paid attention to the research of the photo-Fenton (PF) process. PF occurs in the presence of UV light or visible light with the combination of H_2O_2 and Fe^{2+} or Fe^{3+} to enhance the additional $^{\bullet}OH$ production, thus significantly the Fenton oxidation efficiency [56].

It is worth noting that the difference between the Fenton and the photo-Fenton reaction is that the photo-Fenton could convert Fe^{3+} into Fe^{2+}, and further react to form a weak oxidizing species as superoxide anion radical, CO_2 anion radical and H_2O_2 [57]. In order to enhance photo-Fenton oxidation *via* promoting the conversion of Fe^{3+}/Fe^{2+} and improve the utilization efficiency of H_2O_2, carbonaceous materials, such as graphene oxide-$FePO_4$ (GO-$FePO_4$) [58] are used as organic chelating agents to directly chelate with iron species and donate electrons to accelerate the reaction [59,60]. Cheng *et al.* [61] introduced GO into Fe(III)/H_2O_2 Fenton and photo-Fenton (visible light, $\lambda > 420$ nm) systems to remove chloramphenicol (CAP). As shown in Fig. S1a (Supporting information), different from the researches pointing out that GO acts as iron catalyst support, the GO/Fe(III)/H_2O_2 system showed a higher efficiency (complete removal of CAP within 40 min) with a lower demand of H_2O_2 dosage (0.146 mmol/L), indicating that GO-mediated acceleration of H_2O_2 decomposition *via* the iron activation route enhances the $^{\bullet}OH$ generation for CAP degradation.

Moreover, Du *et al.* [62] have prepared biogenic Fe-Mn oxides (bio-FeMnOx) to catalyze the heterogeneous photo-Fenton for ofloxacin (OFL) degradation. As shown in Fig. S1b (Supporting information), the removal efficiency of OFL was increased significantly from 20% to 98.1% when both H_2O_2 and UV light were present, indicating that e^-/h^+ was generated under photoexcitation and migrated to the surface of bio-FeMnOx. As is shown in Eqs. 4–6, electrons in the valence band are transferred to the conduction band when there is a photoexcitation. Then, the e^-/h^+ pairs could migrate to the catalyst surface and interact with H_2O, OH^-, O_2 and pollutants. Holes and electrons could be the principal contributors to the production of active species and, therefore, may restrain the degradation of OFL.

$$\text{catalyst} + h\gamma \rightarrow h^+_{vb} + e^-_{cb} \quad (4)$$

$$h^+_{vb} + H_2O/OH^- \rightarrow {}^{\bullet}OH + H^+ \quad (5)$$

$$e^-_{cb} + O_2 \rightarrow O_2^{\bullet -} \quad (6)$$

Meanwhile, Fe^{3+}can be transferred to Fe^{2+} with the assistance of photoexcitation, which promotes the Fenton reaction to be generate highly active (Eqs. 7 and 8) [63]. Photogenerated electrons contribute largely to the reduction of Fe^{3+} to Fe^{2+} to ensure the catalytic cycle (Eq. 9) [64].

$$\equiv Fe^{3+} + H_2O + h\gamma \rightarrow Fe^{2+} + {}^{\bullet}OH + H^+ \quad (7)$$

$$\equiv Fe^{2+} + H_2O_2 \rightarrow Fe^{3+} + OH^- + {}^{\bullet}OH \quad (8)$$

$$e^-_{cb} + \equiv Fe^{3+} \rightarrow \equiv Fe^{2+} \quad (9)$$

Recent studies have also shown that suspended particles in water have an impact on antibiotics degradation by UV/H_2O_2. As shown in Fig. S1c (Supporting information), Nie *et al.* [65] systematically investigated the effect of different silica/alumina-based oxide nanoparticles (MCM-41 and Al@MCM-41) in water on the degradation of the antibiotic ofloxacin (OFX) by UV/H_2O_2. The results showed that not only the OFX degradation efficiency but also the reaction rate was greatly enhanced in the presence of Al@MCM-41at a pH range of 3–9, especially at acidic pH values with 84.51% at pH 5.

The mechanism behind the photo-Fenton reaction is to improve the hydroxyl radical generation by a high iron recycle rate to react with H_2O_2 [66,67]. Recent literature has reported that 90%-98% antibiotics can be effectively removed by the solar photo-Fenton method [68,69]. Furthermore, this method also showed promising for the complete elimination of ampicillin (AMP), total cultivable and AMP-resistant *E. coli* and ecotoxicity from secondary-treated wastewater effluents [70]. More specifically, Ferro *et al.* [71] and Fiorentino *et al.* [72], compared the ability of solar/H_2O_2, solar/TiO_2, solar/H_2O_2/TiO_2 and solar photo-Fenton processes for inactivating AMP-resistant *E. coli*, and confirmed that the best disinfection efficiency was obtained by photo-Fenton at pH 4 (Fe^{2+}/H_2O_2: 0.090/0.294 mmol/L). Meanwhile, solar photocatalytic (TiO_2) inactivation efficiency was also very promising, but the recovery of the catalyst after treatment should be taken into count in a global assessment for wastewater reuse application.

2.3. Ozonation process with ex-situ H_2O_2

Ozonation combined with H_2O_2, *i.e.*, the peroxone process, is employed to promote the generation of a large number of $^{\bullet}OH$ [73], which removes a wide range of pollutants from water and wastewater [74,75]. The O_3/H_2O_2 process involves a radical chain mechanism based on ozone decomposition initiated by the hydroperoxide anion $HO_2{}^-$. The synergistic effect of O_3 and H_2O_2 promotes the production of $^{\bullet}OH$, *e.g.*, by the reaction of the H_2O_2 conjugate base (H_2O^-) with ozone generating $^{\bullet}OH$. Initially, O_3 likely reacts with excess $HO_2{}^-$, and the reaction process can be described by Eqs. 10 and 11.

$$H_2O_2 + 2O_3 \rightarrow 2^{\bullet}OH + 3O_2 \tag{10}$$

$$HO_2^- + O_3 \rightarrow {}^{\bullet}OH + O_2^{\bullet-} + O_2 \tag{11}$$

Previous studies indicated that O_3/H_2O_2 could be effective for the mineralization of antibiotics. Chen and Wang [76] investigated the degradation and mineralization of ofloxacin (OFX) by the ozonation and peroxone process. As displayed in Fig. S1d (Supporting information), the mineralization of OFX was significantly enhanced (55%) by the peroxone process, compared to ozonation (30%), though OFX could be rapidly oxidized by both processes. The direct oxidation of OFX by ozone molecules might account for the degradation of OFX in both the ozonation and peroxone process, whereas, in the presence of H_2O_2, the improvement of ozone decomposition and the formation of $^{\bullet}OH$ radicals were responsible for enhancing OFX mineralization. In general, the addition of H_2O_2 to ozonation improves mineralization efficiencies, showing that direct ozone is more prone for antibiotic removal, while intermediate compounds are more deeply degraded by $^{\bullet}OH$.

A series of scientific reports also indicated that the antibiotic mineralization was mainly influenced by the operation conditions such as pH, ozone dosage and temperature. In the O_3/H_2O_2 process, high pH promotes O_3 decomposition by both $^{\bullet}OH$ and $HO_2{}^{\bullet}$ and leads to more $^{\bullet}OH$ production, resulting in a higher TOC removal.

2.4. Ultrasound-enhanced AOPs with ex-situ H_2O_2

Although it has been well known that the Fenton process has been proven to be the most effective AOP for efficient removal of antibiotics from aqueous media, the main drawback of the Fenton reaction is that it is not sustainable due to the slow reduction from Fe^{3+} to Fe^{2+} during the degradation. To improve the effectiveness of Fenton at neutral pH, the combination with ultrasound (US) has attracted great interest [77–79]. US as a very efficient physiochemical technology, which induces the production of sonochemical micro-bubbles in the aqueous system [80,81]. Meanwhile, ultrasonic irradiation of liquids leads to acoustic cavitation in which millions of cavity bubbles form, grow and subsequently implode, resulting in physical and chemical effects [82].

The removal of antibiotics using US/H_2O_2 with heterogeneous catalysts has been widely used to improve the effectiveness of AOPs, especially heterogeneous Fenton-like systems. Ma *et al.* [83] used nanosized zero-valent copper (nZVC) as H_2O_2 activator in conjunction with US for the oxidative degradation of norfloxacin (NOR). Compared with the NOR removal efficiency of 46.68% in nZVC/H_2O_2 system, a significantly enhanced NOR removal of 91.5% was obtained in the US combined Fenton process, which involved a synergistic effect between sonolysis and Fenton-like reaction. The introduction of US obviously avoided the aggregation of the catalyst and changed the physiochemical properties of the catalyst surface [84,85].

Additional related research on AOPs with added H_2O_2 for antibiotics removal are summarized in Table 1 [4,14,17,18,37,44,47,53,62,65,69,70,75,76,84–86]. Specific parameters such as H_2O_2 activator, H_2O_2 dosage, pH and other experimental data have been listed in detail, which can provide guidance for the subsequent removal of various antibiotics in wastewater by AOPs with *ex-situ* H_2O_2.

3. AOPs with *in-situ* production of H_2O_2

3.1. In-situ H_2O_2 production in an electrochemical system

H_2O_2 synthesis by electrochemical oxygen reduction reactions (ORR) has garnered great attention as a green alternative to typical AOPs [87]. Nowadays, the underlying challenge lies in developing materials that exhibit high efficiency and low energy consumption in the electrochemical generation of H_2O_2, favoring the degradation of antibiotics summarized in the following two parts of homogeneous electro-Fenton (homo-EF) and heterogeneous electro-Fenton (hetero-EF).

3.1.1. Homogeneous electro-Fenton process

The electrochemical production of H_2O_2 at the cathode *via* the two-electron ORR (Eq. 12) with the addition of Fe^{2+} induces the common homo-EF process, in which $^{\bullet}OH$ is produced from Fenton's reaction [88–90]. Thus, its practical application for the oxidation of various antibiotics is closely associated with the production of H_2O_2, and the Fe^{2+}/Fe^{3+} cycle.

$$O_{2(g)} + 2H^+ + 2e^- \rightarrow H_2O_2 \tag{12}$$

In these cases, a lot of studies have been focused on cathodic material fabrication and modification as it is one of the main factors determining the efficiency of EF [91,92]. Carbonaceous materials are extensively used as cathode material due to their large surface area, good electrical conductivity, global abundance and low price, especially carbon black [93–95] has been demonstrated to be highly active for two-electron ORR [96–99]. Meanwhile, carbon materials doped with non-metallic elements such as O, N, S and P have been proved high ORR activity and H_2O_2 selectivity, which considered as the promising catalysts [100]. Zhang *et al.* [101] synthesized nitrogen-doped porous carbon (NPC) exhibiting high H_2O_2 selectivity, and achieving a high current efficiency of 87.7% (pH 1, −0.5 V *vs.* SCE). As shown in Fig. 3a, both porous structure and uniform distribution of N accelerated H_2O_2 production and antibiotics degradation, which was valuable for homogeneous EF cathodes with high activity, selectivity and stability.

Table 1
Antibiotics removal by AOPs with *ex-situ* H_2O_2.

Antibiotics	Process based on H_2O_2	H_2O_2 activator	H_2O_2 dosage	pH	Antibiotics removal efficiency (%)	TOC removal (%)	Refs.
Amoxicillin (1 g/L)	Homogeneous Fenton	0.08 g Fe^{2+}	6 mL (3%)	3	80 (70 min)	43	[86]
Ciprofloxacin	Homogeneous Fenton	0.274 g Fe^{2+}	0.8 mL (30% w/w)	3	95 (70 min)	58	[4]
Tetracycline (50 mg/L)	Heterogeneous Fenton	0.3 g/L iron-cobalt oxide nanosheets	20 mmol/L	7	83.5 (50 min)	42.3 (50 min)	[47]
Tetracycline (10 mg/L)	Heterogeneous Fenton	1 g/L FeS nanospheres	15 mmol/L	6	99.6 (3 h)	52.6 (3 h)	[17]
Tetracycline (50 mg/L)	Heterogeneous Fenton	10 mg/L MgNCN/MgO nanocomposites	0.2 mL of 30% H_2O_2	8	>90 (30 min)		[18]
Tetracycline	Heterogeneous Fenton	1 g/L Fe_3O_4@Fe/GA	0.5 mmol/L	6	100 (80 min)	20 (80 min)	[44]
Tetracycline (100 mg/L)	Heterogeneous Fenton	Fe^0/CeO_2 0.1 g/L	100 mmol/L	5.8	93 (60 min)	76.9 (4 h)	[37]
Ofloxacin (30 mg/L)	UV/H_2O_2	UV/biogenic Fe-Mn oxides 5 mg/L	0.04 mmol/L	7	98.1 (2 h)	/	[62]
Oxytetracycline, tetracycline (100 mg/L)	Homogeneous Photo Fenton	UV 0.84 mW/cm/Fe^{2+} 20 mg/L	20 mg/L	7.5	97.1 for both TC and OTC (60 min)	/	[53]
Oxytetracycline (800 µg/L)	UV/pre Fe^0/H_2O_2	UV 6V, Pre-Fe^0 0.3 mmol/L	0.3 mmol/L	7.3	90 (10 min)	82	[14]
Ofloxacin (18 mg/L)	UVA-H_2O_2 induced by suspended particles (Al@MCM-41)	Al@MCM-41 30 mg/L, UVA	1.2 mg/L	7	93.17		[65]
Tetracycline (100 mg/L)	Heterogeneous Photo Fenton	Solar photo, yCeO_2/Fh 0.4 g/L	50 mmol/L	4.0	98.7 (60 min)	70.1	[69]
Ampicillin (100 µg/L)	Solar photo-Fenton oxidation	Solar photo, Fe^{2+} 5 mg/L	50 mg/L	3	99.9 (30 min)	24 (180 min)	[70]
Sulfamethoxazole (0.08 mmol/L)	O_3/H_2O_2	O_3 5.5 mg/min	45.3 µL	7.7	100 (30 min)	83 (3 h)	[75]
Ofloxacin (20 mg/L)	O_3/H_2O_2	O_3 15 mg/L	40 mg/ L	6.7	100 (7 min)		[76]
Norfloxacin (5 mg/L)	US-H_2O_2-catalyst	US 20 kHz/nZVC 0.25 g/L	20 mmol/L	no pH adjustment	91.5 (30 min)	31.8 (30 min)	[84]
Amoxicillin (5 mg/L)	US-H_2O_2-catalyst	US 37 kHz, sea sediment catalyst 4.5 g/L	50 mmol/L	5	98 (60 min)		[85]

Note: GA: graphene aerogel; Al@MCM-41: Al-modified zeolite; nZVC: nanosized zero-valent copper.

In addition to the electrode material, H_2O_2 electro generation is positively correlated with the dissolved O_2 in the aqueous solution. Since the submerged cathode was limited by oxygen transfer in the aqueous solution, it is critical to improve O_2 mass transfer for enhanced ORR performance [102,103]. Li *et al.* [104] proposed a simple electrode aeration (EA) for H_2O_2 electrogeneration, in which gas was directly supplied to the inside of the electrode, after which it diffused to the outside of the electrode, and finally, flowed into the solution. As shown in Fig. 3b, in comparison with the CF using a solution aeration system, the constructed carbon felt with electrode aeration system exhibited a high H_2O_2 generation efficiency and excellent homogeneous EF performance. Several studies have found that the hydrophobic gas diffusion electrode (GDE) can enhance the mass transfer efficiency of oxygen and promote the ORR reaction and H_2O_2 generation [105,106].

It is well known that the use of ligands to promote iron solubility is a preliminary step in the homo-EF process, but the chelation efficiencies of most organic ligands are unsatisfactory, resulting in insufficient availability of Fe^{2+}. In a recent work shown in Fig. 3c, atomic $^{\bullet}$H was introduced to the EF process to accelerate the regeneration of the Fe(II)-complex at a mild pH using a Ni deposited carbon felt (Ni-CF) cathode. The introduction of atomic $^{\bullet}$H significantly elevated total organic carbon (TOC) abatement of CIP from 42% (CF) to 81% (Ni-CF) at a neutral pH [107]. As shown in Table S1 (Supporting information), more related studies on the homo-EF with the *in-situ* production of H_2O_2 for antibiotics removal is summarized.

3.1.2. Heterogeneous electro-Fenton process

Although the homo-EF has been extensively applied for the degradation of various types of antibiotics, two obvious disadvantages remain, which are limiting its wide application: (i) The process is only optimum at strong acidic pH condition (*i.e.*, pH 2.8–3.5), and (ii) the catalyst cannot be recycled [108]. Therefore, heterogeneous electro-Fenton (hetero-EF) is a promising alternative to homo-EF to overcome the above disadvantages [109,110].

Over the past few years, most Fe-based natural or synthetic solid catalysts have been utilized as heterogeneous catalysts in the EF process for the decomposition of H_2O_2 to $^{\bullet}$OH, such as α-FeOOH [111], FeS [112] and Pd/Fe_3O_4 [113]. However, the agglomeration of the nanoparticles reduces the efficiency of the hetero-EF catalysis. Recent research has reported that core–shell structured catalysts containing a transition metal nanoparticle core and a graphitized porous carbon shell show remarkably enhanced catalytic activity and stability [114], especially MOFs-derived metal incorporated carbons [115]. As shown in Fig. 3d, Du *et al.* [116] synthesized Fe-based nanoparticles with porous carbon (Fe/Fe_3C@PC) core–shell structured hybrid through one-pot pyrolysis of MIL-101(Fe) and used them as an efficient hetero-EF catalyst for SMT degradation.

Nowadays, the emergence of co-catalysts offers a new prospect for the further development of AOPs [117,118]. In recent years various kinds of organic and inorganic materials have been added as co-catalyst to enhance the generation of $^{\bullet}$OH [119,120]. Tian *et al.* [121] compared the degradation of SMT by Fe^0 and Fe^0/MoS_2

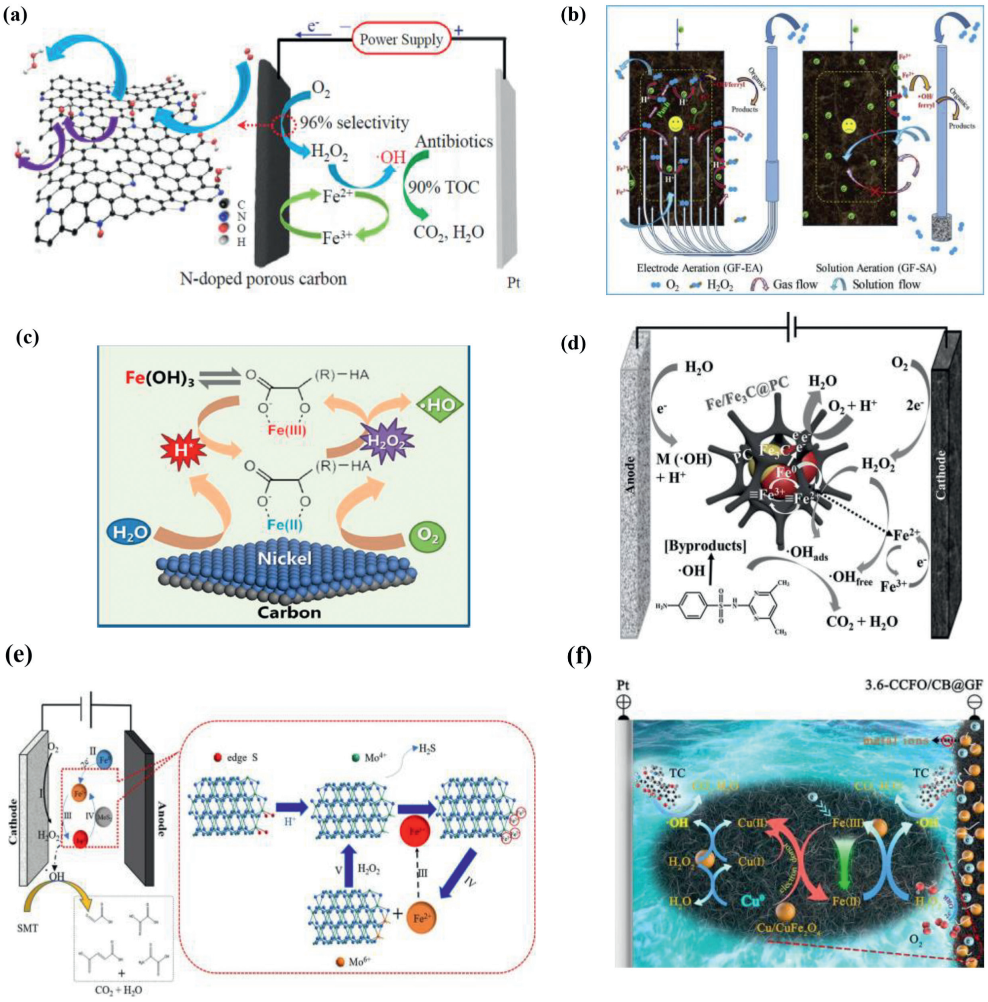

Fig. 3. (a) Mechanism of N-doped porous carbon cathode *in situ* high-selectivity production of hydrogen peroxide and degradation of antibiotics. Copied with permission [101]. Copyright 2020, Elsevier. (b) The enhanced Electro-Fenton degradation mechanism of CF-EA. Copied with permission [104]. Copyright 2020, Elsevier. (c) Reaction mechanism for CIP degradation by using Ni-CF cathode introduced atomic $^{\bullet}$H for H_2O_2 activation. Copied with permission [130]. Copyright 2019, American Chemical Society. (d) The proposed scheme of mechanism of the Hetero-EF process catalyzed by Fe/Fe_3C@PC catalyst. Copied with permission [116]. Copyright 2020, Elsevier. (e) The proposed enhancement mechanism of the MoS_2 co-catalyst heterogenous Fe^0-EF process for SMT degradation. Copied with permission [121]. Copyright 2021, Elsevier. (f) Mechanisms for TC degradation by 3.6-CCFO/CB@GF systems. Copied with permission [129]. Copyright 2021, Elsevier.

hetero-EF process, confirming the latter could enhance the rate constant by twofold, compared to the Fe^0-EF process under the same optimal conditions. As shown in Fig. 3e, due to co-catalysis's characteristics, MoS_2 could greatly facilitate the Fe^{3+}/Fe^{2+} recycle reaction by the exposed Mo^{4+} active sites, which significantly promoted the decomposition of H_2O_2 that generated in Fe^0-EF system and improved the generation of hydroxyl radicals.

Until now, hetero-EF, which utilizes functionalized cathodes has primarily focused on iron-fixed carbon supports, including Fe_3O_4@Fe_2O_3/activated carbon aerogel cathode [122], Fe_3O_4/GDE [123], Fe^0-in-carbon nanotubes (CNTs) [124] and Fe_3O_4/graphite felt [125]. Notably, the introduction of other transition metals into the structure of iron minerals to fabricate binary-oxide composite electrodes (*e.g.*, FeCu/carbon aerogel [126], Mn/Fe@ porous carbon [127], and Cu-doped Fe@Fe_2O_3/nickel foam [128]) has been tested as a strategy to boost the cathode's electron transfer efficiency. Cui *et al.* [129] investigated the hetero-EF catalytic behavior of Cu/$CuFe_2O_4$/CB@GF as shown in Fig. 3f, which possessed wide pH applicability (3–7) to TC degradation and maintained 80% removal after five consecutive runs. Besides, other more recent studies related to hetero-EF for degradation of antibiotics are outlined in Table S2 (Supporting information).

3.2. In-situ H_2O_2 production in photo-electrochemical systems

The efficient decomposition of H_2O_2 into $^{\bullet}$OH is one of the decisive factors influencing the degradation efficiency of antibiotics. In the EF process, light irradiation is helpful for the generation of $^{\bullet}$OH with the semiconductor catalyst, since the photo-induced electrons can promote the decomposition of H_2O_2 [131]. Besides, the photo-induced electron-hole pairs (e^--h^+) on the semiconductor are also beneficial for the generation of active species such as $^{\bullet}$OH and $O_2^{\bullet -}$ radicals [132]. The synergetic excitation of multiple active species promotes the decomposition of organic contaminants. Therefore, the photo-electrochemical (PEC) system especially photo-electro-Fenton (PEF) process shows great potential in antibiotics removal.

Jia *et al.* [133] reported a novel Fe-free PEF system for CIP degradation. As shown in Fig. S3a (Supporting information), a sensible heterogeneous PEF degradation mechanism was proposed, the MnOx formed solid heterojunction interface on g-C_3N_4 nanosheets stably ensured the fast separation and transfer of charges. A series of experimental data showed that a coexistence of $^{\bullet}$OH, $^{\bullet}O_2^-$, h^+ and e^- in the PEF process and the $^{\bullet}$OH played the principal role in the degradation of CIP. Compared with the traditional Fenton reaction, the PEF system also showed an expanded range of pH 2–

7, whose CIP degradation efficiency remained at 80.31% when pH was 7. Moreover, the catalyst also showed excellent stability with degradation efficiency of 91.62% after four consecutive runs. Therefore, the photoelectric synergy system with the polyvalent manganese was a promising approach in treating organic contaminants in water.

3.3. In-situ H_2O_2 production in bioelectrochemical system

Although H_2O_2 based AOPs have been considered a promising method to remove various antibiotics, the cost of H_2O_2 and its risk in transport and use may be the main restrictions for application [134]. To solve the problem, many recent studies have considered that bio-electrochemical systems (BESs) are low-cost and environment friendly technologies for H_2O_2 synthesis, including microbial electrolysis cells (MECs) [135] and microbial fuel cells (MFCs) [136].

Recently, *in-situ* H_2O_2 generating BESs were coupled with EF-based AOPs, and have been verified as a promising technique to deal with antibiotics removal [137–139]. In such cases, H_2O_2 is continuously generated *in-situ* in the cathodic chamber by coupling anodic oxidation of organic compounds (electricity production). Thereby no external power input is needed as opposed to the conventional EF or PEF methods. Furthermore, the H_2O_2 produces $^{\bullet}OH$ by the external supplement of an iron source to oxidize recalcitrant organics [140], which was shown effective for the degradation of several common antibiotics such as penicillin [141], TC [142] and erythromycin [143].

As well known, most of the conventional microbial oxidation reactions of *in-situ* H_2O_2 generating BESs in the anode chamber are usually low-cost and self-sustaining. Electrochemical active bacteria are firstly used to oxidize electron donors [144], then the electrons transfer directly through an external circuit to the cathode for H_2O_2 production [145–147]. Meanwhile, Fe^{2+} is generated *in-situ* at neutral pH by direct electro-reduction of iron oxide in the cathode chamber. A BEF system does not only produce $^{\bullet}OH$ radicals in the cathodic chamber for antibiotics degradation but also generates electricity [142].

However, the exposure to antibiotics in the anode chamber leads to harboring abundant antibiotic resistance genes (ARGs), and the abundance might be increased with operation time, thus increasing attention has been paid to efficiently remove recalcitrant antibiotics in the cathode chamber using BESs. Besides, the iron source plays a critical role to catalyze the Fenton oxidation in the BESs. Recently, several studies have focused on heterogeneous iron salts as Fenton catalyst in BES, including synthesized and/or natural iron oxides, such as lepidocrocite (γ-FeOOH), maghemite (γ-Fe_2O_3), clino-pyrrhotite ($Fe_{1-x}S$), limonite (FeOOH), iron vanadate ($FeVO_4$), iron phthalocyanine (FePc), Fe@ Fe_2O_3 [148].

Wang *et al.* [149] investigated the removal of three veterinary antibiotics *i.e.*, TC, tylosin and sulfaquinoxaline in a set of a H-type MEF system catalyzed by a novel M-type strontium hexaferrite nanoparticles (SrM-NPs) as heterogeneous Fenton catalyst as shown in Fig. S3b (Supporting information). The system resulted in degrading 85.9%-88.2% of 10 mg/L antibiotics in 17 h, and complete degradation occurred within 24 h with a TOC removal of 74%-87%. Conversely, 20% lower degradation of antibiotics was attained using a homogeneous Fenton catalyst (*i.e.*, $FeSO_4$). The system reached a maximum current and power output of 241 ± 10.9 mA/m^2 and 136.4 ± 3.1 mW/m^2, respectively, which exhibited a promising and energy-efficient approach for the degradation of antibiotics. Nevertheless, the technology still faces some drawbacks at the present stage, such as low H_2O_2 yield, low unit cell body throughput, low current density and low conductivity [150]. Nevertheless, the Fenton/ Fenton-like process based on microbial fuel cells offers a green and sustainable solution for wastewater treatment along with power production and utilization.

3.4. In-situ H_2O_2 production in photochemical systems

Nowadays, photocatalytic production of H_2O_2 from water and O_2 has received increasing attention as a sustainable and eco-friendly alternative to other methods such as anthraquinone oxidation, alcohol oxidation, and electrochemical synthesis because it can *in-situ* produce H_2O_2 and then effective photodegrade antibiotics and other organic pollutants into harmless products simultaneously [151–153]. According to the literature, the photochemical production of H_2O_2 can be divided into homogeneous photo-Fenton and heterogeneous photo-Fenton processes.

3.4.1. Homogeneous photo-Fenton process

This novel photo-Fenton process is usually performed in the presence of Fe^{3+}, ligands (L), O_2 and light irradiation [154]. Previous studies have shown that the complexes formed with Fe^{3+} could produce both Fe^{2+} and ligand-free radicals by ligand-to-metal charge transfer (LMCT) under irradiation as shown in Eq. 13. Then the ligand-free radical is able to react with dissolved oxygen in water to form $O_2^{\bullet-}$ as displayed in Eqs. 14 and 15. The $O_2^{\bullet-}$ radical and its conjugated acid form $HO_2^{\bullet-}$, which can participate in further reactions generating H_2O_2. As a consequence, $^{\bullet}OH$ can be formed by the Fenton reaction.

$$\mathrm{Fe(III)-L} + h\gamma \rightarrow [\mathrm{Fe(III)-L}]^{\bullet} \rightarrow \mathrm{Fe(II)} + \mathrm{L}^{\bullet} \tag{13}$$

$$\mathrm{L}^{\bullet} + \mathrm{O_2} \rightarrow \mathrm{O_2^{\bullet-}} + \mathrm{L} \tag{14}$$

$$\mathrm{O_2^{\bullet-}} + \mathrm{H^+} \leftrightarrow \mathrm{HO_2^{\bullet-}} \tag{15}$$

3.4.2. Heterogeneous photo-Fenton process

In the heterogeneous photo-Fenton (HPF) process based on the activation of O_2, the *in-situ* generation of H_2O_2 can be realized by the reaction of dissolved O_2 with the photo-generated electrons from semiconductors under light irradiation, then it can be decomposed to $^{\bullet}OH$ through homogeneous or heterogeneous Fe-based catalysts for the degradation of contaminants [69,155]. In this novel photo-Fenton process, the *in-situ* generation of H_2O_2 by the activation of O_2 is the prerequisite, which depends on the properties of the semiconductor, the light irradiation and the supply mode of O_2.

$$\mathrm{catalyst} + h\gamma \rightarrow \mathrm{h^+} + \mathrm{e^-} \tag{16}$$

$$2\mathrm{h^+} + 2\mathrm{H_2O} \rightarrow \mathrm{H_2O_2} + 2\mathrm{H^+} \tag{17}$$

$$2\mathrm{H^+} + \mathrm{O_2^{\bullet-}} + \mathrm{e^-} \rightarrow \mathrm{H_2O_2} \tag{18}$$

$$\mathrm{HO^{\bullet}/O_2^{\bullet-}/h^+} + \mathrm{antibiotics} \rightarrow \mathrm{degradation\ products} \tag{19}$$

So far, iron catalysts supported on g-C_3N_4 [152,156–161], TiO_2 [153], $BiVO_4$ [162,163], MOFs and other porous materials have been studied extensively as potential catalysts for photocatalytic production of H_2O_2 [164]. The synthesis strategies of iron catalysts supported on these semiconductors are focused on iron species in different states, from lattice doping and single-atom sites, to surface amorphous/crystalline nanoparticles, and further to heterojunctions [165]. TiO_2 and BiOCl are wide band-gap semiconductors that can only respond to UV light, while g-C_3N_4 and iron-containing MOFs are normally narrow band-gap semiconductors that are visible light responsive.

Table S3 (Supporting information) lists the recent studies for antibiotics removal in wastewater by the HPF processes. Although these novel HPF processes have been widely applied for the degradation of inorganic and organic pollutants due to the Fenton process without the addition of H_2O_2 and the reduction of Fe^{3+} to Fe^{2+} by the photoelectrons, several drawbacks are still required to overcome, such as the low utilization rate of light energy, low on-site production efficiency of H_2O_2, high operational costs and design of photo-reactor, which will limit the development of this HPF on a large scale.

To satisfy the practical application requirements regarding efficiency and universality, many Fenton-like photocatalysts are constructed by anchoring metal ions or compounds on the surface of photocatalysts [166]. This does not only broaden the pH range of the reaction and eliminate the problem of removing soluble iron ions, but also assists the photocatalysts to generate H_2O_2 by the reduction of oxygen [167–170]. Gao *et al.* [162] reported the photoactivity of Fe^{3+} grafted $BiVO_4$ photocatalyst by the visible light photodegradation of various antibiotics. Following the mechanism shown in Fig. S3c (Supporting information), the Fe^{3+} species do not only serve as efficient electron trapping centers to inhibit recombination of photogenerated charges and activate molecular oxygen as shown in Eqs. 16–19, but also dramatically enhance the surface area of the photocatalyst, providing more reaction sites. Notably, the degradation rate of 7% Fe^{3+}-BVO photocatalyst after light irradiation for 10 min reached 80%, which was 63% higher than for pure BVO.

4. Application for antibiotics removal from wastewater

According to the structural characteristics of antibiotics, they can be mainly divided into quinolones, imidazole, tetracyclines, sulfamic acid and lactone rings [171]. After the previous summary of this review, we can conclude that the majority of antibiotics can be effectively removed by H_2O_2-based AOP processes. Among them, tetracyclines, sulfonamides, quinolones and chloramphenicol antibiotics are most often used as target pollutants. However, at present, metronidazole antibiotics cannot be degraded by a single AOP based on H_2O_2, but the combined AOPs can effectively treat metronidazole antibiotics (details will be introduced later).

In most cases, only one approach is used for antibiotics removal. However, the actual sewer system wastewater is relatively complicated containing various antibiotics. Herein, combined methods may be more efficient than a single method. Recent literature has shown that the integration of two or more treatment methods may help circumvent the limitations that a typical single process presents during the degradation of antibiotics. Pan *et al.* [14] investigated the novel UV/pre-Fe^0/H_2O_2 system to remove several antibiotics classes from secondary wastewater effluents (SWE). As shown in Fig. S4a (Supporting information), the corrosion of Fe^0 is enhanced by magnetization based on the “magnetic memory” of iron [28]. An outstanding mineralization rate was demonstrated for various antibiotics from SWE at neutral pH with a TOC removal of 92.1%, while for UV/H_2O_2 and UV/Fe^0/H_2O_2 system it was 53.9% and 72.1%, respectively. To sum up, the UV/pre- Fe^0/H_2O_2 combined process is a promising and cost-effective for the treatment of antibiotics in SWE.

In addition to the photo-assisted catalysts for antibiotics removal, photo-assisted MFC are also used to simultaneously generate and activate H_2O_2 to promote the rapid degradation of antibiotics. As described in Fig. S4b (Supporting information), Mo and W catalytic species immobilized onto a graphite felt cathode did not only enhance the cathodic reduction of metronidazole (MNZ) under anaerobic conditions, but also intensified the oxidation of MNZ under aerobic conditions, which further accelerated in the presence of Fe^{3+} in this combined system. Meanwhile, photogenerated holes were directly involved into the oxidation of MNZ under anaerobic conditions. This study demonstrates the efficiency of the combination of photo-assisted MFCs and a Fenton-MFCs process for the intensification of the removal of antibiotics with simultaneous production of renewable electrical energy.

Coupling electrochemical processes with physical (*e.g.*, membrane filtration) [172], chemical (*e.g.*, ionizing radiation, enzymatic oxidation) [173], or biological (*e.g.*, anaerobic fermentation) [174,175] methods can expand the applicability of these processes to more complex matrices, enhance the efficiency of mineralization, avoid the formation of toxic by-products, and reduce the operating costs of the antibiotics degradation systems [172,175–178]. Jiang *et al.* [179] prepared a novel graphene modified electro-Fenton catalytic membrane (EFCM) for *in situ* degradation of the antibiotic florfenicol in low concentration. The degradation mechanism is shown in Fig. S4c (Supporting information), EFCM acted not only as a cathode for EF oxidation in a continuous mode but also as a membrane barrier to concentrate and enhance the mass transfer of florfenicol, which increased its oxidation chances. Similarly, Guo *et al.* [180] have developed a silicate-enhanced flow-through electro-Fenton system with Fe_2O_3 catalysts confined within CNTs. The composite filter system demonstrated an improved *in-situ* H_2O_2 generation yield to produce more reactive oxygen species, thus significantly boosting the reaction kinetics and desirable catalyst stability. The above results collectively highlighted the feasibility of the combined membrane filtration – H_2O_2-based oxidation process for advanced water purification. Other more recent studies related to the application of combined processes for the treatment of antibiotics are outlined in Table S4 (Supporting information).

5. Conclusions and future perspectives

The H_2O_2-based AOPs have proven effective for detoxifying a wide range of antibiotics in wastewater. Various H_2O_2-based AOP processes, including AOPs that require H_2O_2 addition and the AOPs with *in-situ* production of H_2O_2, are discussed. This study reviewed various antibiotic removal strategies, focusing on the performance and corresponding mechanisms.

Although numerous approaches have been reported to remove antibiotics, most of them have some neglected disadvantages, hence this process still requires further research for its commercial applications and several challenges remain in this intriguing field. In order to meet the highly competitive requirements of antibiotics removal in actual wastewater in the future, main emphasis towards H_2O_2-based AOPs should be put in the following aspects.

(1) The main challenges encountered in AOPs with added H_2O_2 are the limited H_2O_2 activation efficiency. Although the optimization of heterogeneous catalysts, photolysis, O_3 and ultrasonic assistance has been widely used to enhance the utilization efficiency of H_2O_2 for improving antibiotics degradation in wastewater, there are still few studies on the mechanism of free radical formation and transformation, development of rate expressions, and identification of scale-up parameters. Meanwhile, more research works should be focused on the stability and cost of catalysts, H_2O_2 utilization rate, and total energy consumption during the antibiotics degradation in wastewater, to evaluate the technical and economic feasibility of the process.

(2) The efficiency of EF-based processes is highly dependent on the synthesis of H_2O_2. However, development of electrochemical production of H_2O_2 is still challenging because of the low H_2O_2 yield and unsatisfactory current efficiency mainly deriving from the catalytic activity and selectivity of catalysts. Moreover, GDE in recent research still requires additional aeration, reducing electrode usage while generating extra energy consumption. Thus, future studies need to focus not only on improving cata-

lyst and reactor design but also on the reaction process at the electrode interface to improve the utilization efficiency of oxygen.

(3) In the photo-Fenton process based on the activation of O_2, photocatalysts with long-term stability and with visible light response performance should continue to be developed. Special attention should be paid to the photo-catalysts composed of semiconductor, iron and carbon, because carbonaceous materials can promote the production of H_2O_2 and the photoelectrons can enhance the conversion of Fe^{3+} to Fe^{2+}, which will favor the utilization of H_2O_2. Moreover, the synthesis of photocatalysts that have a narrow band gap and efficient activity under visible light needs to be further developed for more industrial applications under solar light. In addition, the removal of catalysts after treatment should be taken into account in a global assessment for wastewater reuse application.

(4) Hybrid methods are economically viable techniques for the treatment of a wide range of industrial effluents. Also, the capital cost for reactors and other accessories can be reduced since one reactor can simultaneously generate and consume H_2O_2 *in-situ* and remove pollutants without the need of multiple reactors. The use of a combined process decreases the operational costs related to energy consumption, and enhances $^{\bullet}OH$ availability and treatment efficiency. Further research should aim to improve the efficiency at wide pH ranges, application with real wastewaters, strategies to apply this approach in pilot scale studies and implementing a synergistic approach between anodic and cathodic environment. It is also essential to carry out more studies on more types of antibiotic resistant bacteria and viruses as good results have been shown in previous studies. Finally, studies in real and natural contaminated water are required for the actual application of this process. Future studies should focus on the cost-effectiveness of H_2O_2-based AOPs and explore the actual amount of energy consumed over the other conventional treatment methods. It is necessary to carry out more pilot-scale experiments with real industrial wastewater for the identification of scale-up parameters.

Declaration of competing interest

We declare that we have no financial and personal relationships with other people or organizations that can inappropriately influence our work, there is no professional or other personal interest of any nature or kind in any product, service and/or company that could be construed as influencing the position presented in, or the review of, the manuscript entitled.

Acknowledgments

This work was financially supported by National Natural Science Foundation of China (Nos. 21976096, 52170085 and 21773129), Tianjin Development Program for Innovation and Entrepreneurship, Key Project of Natural Science Foundation of Tianjin (No. 21JCZDJC00320), Tianjin Post-graduate Students Research and Innovation Project (No. 2021YJSB013), and Fundamental Research Funds for the Central Universities, Nankai University.

Supplementary materials

Supplementary material associated with this article can be found, in the online version, at doi:10.1016/j.cclet.2022.06.044.

References

[1] X. Liu, S. Lu, W. Guo, B. Xi, W. Wang, Sci. Total Environ. 627 (2018) 1195–1208.
[2] M. Qiao, G.G. Ying, A.C. Singer, Y.G. Zhu, Environ. Int. 110 (2018) 160–172.
[3] S. Li, W. Shi, M. You, et al., Environ. Pollut. 246 (2019) 435–442.
[4] T. Mackuľak, K. Nagyová, M. Faberová, et al., Environ. Toxicol. Pharmacol. 40 (2015) 492–497.
[5] A. Kumar, D. Pal, J. Environ. Chem. Eng. 6 (2018) 52–58.
[6] X. Liu, F. Huang, Y. Yu, et al., Chemosphere 226 (2019) 103–109.
[7] M.A. De León, J. Castiglioni, J. Bussi, M. Sergio, Catal. Today 133-135 (2008) 600–605.
[8] R. Rosal, A. Rodríguez, J.A. Perdigón Melón, et al., Water Res. 42 (2008) 3719–3728.
[9] Y. Chen, J. Yang, L. Zeng, M. Zhu, Crit. Rev. Environ. Sci. Technol. 52 (2022) 1401–1448.
[10] B.L. Phoon, C.C. Ong, M.S. Mohamed Saheed, et al., J. Hazard. Mater. 400 (2020) 122961.
[11] J. Wang, R. Zhuan, Sci. Total Environ. 701 (2020) 135023.
[12] A.J. dos Santos, M.S. Kronka, G.V. Fortunato, M.R.V. Lanza, Curr. Opin. Electrochem. 26 (2021) 100674.
[13] X. Du, M.A. Oturan, M. Zhou, et al., Appl. Catal. B: Environ. 296 (2021) 120332.
[14] Y. Pan, Y. Zhang, M. Zhou, J. Cai, Y. Tian, Water Res. 153 (2019) 144–159.
[15] Y. Wang, H. Zhao, M. Li, J. Fan, G. Zhao, Appl. Catal. B: Environ. 147 (2014) 534–545.
[16] Y. Pan, M. Zhou, X. Li, et al., Sep. Purif. Technol. 169 (2016) 83–92.
[17] X.C. Wang, Y. Zhuang, J. Zhang, L.Z. Song, B.Y. Shi, Sci. Total Environ. 714 (2020) 136436.
[18] L. Ge, Y. Yue, W. Wang, et al., Water Res. 198 (2021) 117149.
[19] M. Kallel, C. Belaid, R. Boussahel, et al., J. Hazard. Mater. 163 (2009) 550–554.
[20] T. Zhou, Y. Li, J. Ji, F.S. Wong, X. Lu, Sep. Purif. Technol. 62 (2008) 551–558.
[21] X. Li, Y. Huang, C. Li, J. Shen, Y. Deng, Chem. Eng. J. 260 (2015) 28–36.
[22] L. Guo, F. Chen, X. Fan, W. Cai, J. Zhang, Appl. Catal. B: Environ. 96 (2010) 162–168.
[23] T. Zhou, X. Wu, J. Mao, Y. Zhang, T.T. Lim, Appl. Catal. B: Environ. 160-161 (2014) 325–334.
[24] H.N. Che, X. Gao, J. Chen, et al., Angew. Chem. Int. Ed. 60 (2021) 25546–25550.
[25] M. Munoz, Z.M. de Pedro, J.A. Casas, J.J. Rodriguez, Appl. Catal. B: Environ. 176-177 (2015) 249–265.
[26] Y. Pan, H. Guo, M. Zhou, et al., Chem. Eng. J. 372 (2019) 905–916.
[27] Y. Pan, M. Zhou, J. Cai, et al., Chem. Eng. J. 339 (2018) 411–423.
[28] Y. Pan, Y. Zhang, M. Zhou, et al., Chem. Eng. J. 354 (2018) 777–789.
[29] Y. Zhang, M. Zhou, J. Hazard. Mater. 362 (2019) 436–450.
[30] Y. Zhang, N. Klamerth, P. Chelme-Ayala, M. Gamal El-Din, Environ. Sci. Technol. 50 (2016) 10535–10544.
[31] J. He, X. Yang, B. Men, L. Yu, D. Wang, J. Mol. Catal. A: Chem. 408 (2015) 179–188.
[32] T. Zhou, K. Feng, W. Xiang, et al., Chemosphere 193 (2018) 968–977.
[33] T. Zhou, Y. Li, F.S. Wong, X. Lu, Ultrason. Sonochem. 15 (2008) 782–790.
[34] Y. Pan, Z. Bu, C. Sang, et al., Sep. Purif. Technol. 250 (2020) 117281.
[35] Y.Q. Cong, Z. Li, Y. Zhang, Q. Wang, Q. Xu, Chem. Eng. J. 191 (2012) 356–363.
[36] F.C.C. Moura, M.H. Araujo, R.C.C. Costa, et al., Chemosphere 60 (2005) 1118–1123.
[37] N. Zhang, J. Chen, Z. Fang, E.P. Tsang, Chem. Eng. J. 369 (2019) 588–599.
[38] B. Yuan, J. Xu, X. Li, M.L. Fu, Chem. Eng. J. 226 (2013) 181–188.
[39] X. Zhang, W. Guo, H.H. Ngo, et al., J. Environ. Manag. 172 (2016) 193–200.
[40] V.T. Nguyen, T.B. Nguyen, C.W. Chen, et al., Bioresour. Technol. 284 (2019) 197–203.
[41] J. Zhou, F. Ma, H. Guo, D. Su, Appl. Catal. B: Environ. 269 (2020) 118784.
[42] Y. Zhuang, Q.Z. Liu, Y. Kong, et al., Environ. Sci. Nano 6 (2019) 388–398.
[43] Y. Zhuang, X.C. Wang, Q.Z. Liu, B.Y. Shi, Chem. Eng. J. 379 (2020) 122310.
[44] Y. Zhuang, X.C. Wang, L.L. Zhang, D.D. Dionysiou, B.Y. Shi, Environ. Sci. Nano 6 (2019) 3232–3241.
[45] J. Zhang, S. Qiu, H. Feng, et al., Chem. Eng. J. 428 (2022) 131403.
[46] Y. Tian, X. He, H. Zhou, et al., Chemosphere 257 (2020) 127209.
[47] M. Nie, Y. Li, L. Li, et al., Appl. Surf. Sci. 535 (2021) 147655.
[48] Y. Zhuang, X.C. Wang, L.L. Zhang, D.D. Dionysiou, Environ. Sci. Nano 6 (2019) 3232–3241.
[49] K. Lekkerkerker-Teunissen, M.J. Benotti, S.A. Snyder, H.C. van Dijk, Sep. Purif. Technol. 96 (2012) 33–43.
[50] Y.J. Jung, W.G. Kim, Y. Yoon, et al., Sci. Total Environ. 420 (2012) 160–167.
[51] A. Zuorro, M. Fidaleo, M. Fidaleo, R. Lavecchia, J. Environ. Manag. 133 (2014) 302–308.
[52] Y. Liu, X. He, Y. Fu, D.D. Dionysiou, Chem. Eng. J. 284 (2016) 1317–1327.
[53] C.H. Han, H.D. Park, S.B. Kim, et al., Water Res. 172 (2020) 115514.
[54] Y. Chen, C. Hu, X.X. Hu, J.H. Qu, Environ. Sci. Technol. 43 (2009) 2760–2765.
[55] S. He, M. Shen, E. Wu, et al., Environ. Sci. Ecotechnol. 9 (2022) 100141.
[56] A. Sharma, J. Ahmad, S.J.S. Flora, Environ. Res. 167 (2018) 223–233.
[57] F.C. Moreira, R.A.R. Boaventura, E. Brillas, V.J.P. Vilar, Appl. Catal. B: Environ. 202 (2017) 217–261.
[58] S. Guo, G. Zhang, J.C. Yu, J. Colloid Interface Sci. 448 (2015) 460–466.
[59] R. Liu, Y. Xu, B. Chen, Environ. Sci. Technol. 52 (2018) 7043–7053.
[60] Y. Liu, W. Jin, Y. Zhao, G. Zhang, W. Zhang, Appl. Catal. B: Environ. 206 (2017) 642–652.
[61] F. Cheng, P. Zhou, Y. Liu, et al., Sci. Total Environ. 797 (2021) 149097.
[62] Z. Du, K. Li, S. Zhou, et al., Chem. Eng. J. 380 (2020) 122427.
[63] Q. Wang, B. Wang, Y. Ma, S. Xing, Chem. Eng. J. 354 (2018) 473–480.
[64] W. Du, Y. Xu, Y. Wang, Langmuir 24 (2008) 175–181.
[65] Y. Nie, X. Sun, M. Wang, et al., J. Hazard. Mater. 412 (2021) 125259.
[66] P. García-Muñoz, N.P. Zussblatt, G. Pliego, et al., J. Environ. Manag. 238 (2019) 243–250.

[67] S.K. Mondal, A.K. Saha, A. Sinha, J. Clean. Prod. 171 (2018) 1203–1214.
[68] M.B. Ahmed, J.L. Zhou, H.H. Ngo, W. Guo, Sci. Total Environ. 532 (2015) 112–126.
[69] X. Huang, N. Zhu, F. Mao, et al., Chem. Eng. J. 392 (2020) 123636.
[70] L. Ioannou-Ttofa, S. Raj, H. Prakash, D. Fatta-Kassinos, Chem. Eng. J. 355 (2019) 91–102.
[71] G. Ferro, A. Fiorentino, M.C. Alferez, et al., Appl. Catal. B: Environ. 178 (2015) 65–73.
[72] A. Fiorentino, G. Ferro, M.C. Alferez, et al., J. Photochem. Photobiol. B 148 (2015) 43–50.
[73] J. Wang, S. Wang, J. Environ. Manag. 182 (2016) 620–640.
[74] J. Gomes, R. Costa, R.M. Quinta-Ferreira, R.C. Martins, Sci. Total Environ. 586 (2017) 265–283.
[75] J. Martini, C.A. Orge, J.L. Faria, M.F.R. Pereira, O.S.G.P. Soares, J. Environ. Chem. Eng. 6 (2018) 4054–4060.
[76] H. Chen, J. Wang, Chemosphere 269 (2021) 128775.
[77] C.H. Weng, Y.T. Lin, H.M. Yuan, Sep. Purif. Technol. 117 (2013) 75–82.
[78] C.H. Weng, V. Huang, J. Ind. Eng. Chem. 28 (2015) 153–160.
[79] M. Cai, J. Su, G. Lian, et al., Ultrason. Sonochem. 31 (2016) 193–200.
[80] Y. Dai, F. Li, F. Ge, et al., J. Hazard. Mater. 137 (2006) 1424–1429.
[81] B. Chen, X. Wang, C. Wang, W. Jiang, S. Li, Ultrason. Sonochem. 18 (2011) 1091–1096.
[82] K. Ninomiya, H. Takamatsu, A. Onishi, K. Takahashi, N. Shimizu, Ultrason. Sonochem. 20 (2013) 1092–1097.
[83] L. Hou, L. Wang, S. Royer, H. Zhang, J. Hazard. Mater. 302 (2016) 458–467.
[84] X. Ma, Y. Cheng, Y. Ge, et al., Ultrason. Sonochem. 40 (2018) 763–772.
[85] F. Damiri, S. Dobaradaran, S. Hashemi, et al., Ultrason. Sonochem. 68 (2020) 105187.
[86] R.X. Guo, X.D. Xie, J.Q. Chen, Environ. Technol. 36 (2015) 844–851.
[87] J. Li, Y. Li, Z. Xiong, G. Yao, B. Lai, Chin. Chem. Lett. 30 (2019) 2139–2146.
[88] E. Brillas, I. Sirés, M.A. Oturan, Chem. Rev. 109 (2009) 6570–6631.
[89] J.F. Pérez, J. Llanos, C. Sáez, et al., Electrochem. Commun. 89 (2018) 19–22.
[90] Z. Xu, L. Qin, Y. Zhang, et al., J. Hazard. Mater. 369 (2019) 299–308.
[91] R. Babaei-Sati, J. Basiri Parsa, J. Ind. Eng. Chem. 52 (2017) 270–276.
[92] E.C. Paz, L.R. Aveiro, V.S. Pinheiro, et al., Appl. Catal. B: Environ. 232 (2018) 436–445.
[93] Z. Wang, Q.-K. Li, C. Zhang, et al., ACS Catal. 11 (2021) 2454–2459.
[94] C. Xia, Y. Xia, P. Zhu, L. Fan, H. Wang, Science 366 (2019) 226–231.
[95] X.C. Wang, B.S. Liu, B.Y. Shi, et al., Desalin. Water Treat. 168 (2019) 348–356.
[96] K. Jiang, S. Back, A.J. Akey, et al., Nat. Commun. 10 (2019) 3997.
[97] R. Shen, W. Chen, Q. Peng, et al., Chem 5 (2019) 2099–2110.
[98] E. Jung, H. Shin, B.-H. Lee, et al., Nat. Mater. 19 (2020) 436–442.
[99] Z. Lu, G. Chen, S. Siahrostami, et al., Nat. Catal. 1 (2018) 156–162.
[100] S.Y. Chen, T. Luo, K.J. Chen, et al., Angew. Chem. Int. Ed. 60 (2021) 16607–16614.
[101] D. Zhang, T. Liu, K. Yin, C. Liu, Y. Wei, Chem. Eng. J. 383 (2020) 123184.
[102] H.C. Zhang, Y.J. Li, H. Zhang, G.H. Li, F. Zhang, Sci. Rep. 9 (2019) 1817.
[103] A.Y. Kupryazhkin, A.N. Zhiganov, D.V. Risovanyi, V.D. Risovanyi, V.N. Golovanov, Tech. Phys. 49 (2004) 254–257.
[104] D. Li, T. Zheng, Y. Liu, et al., J. Hazard. Mater. 396 (2020) 122591.
[105] H.C. Zhang, Y.S. Zhao, Y.J. Li, et al., ACS Appl. Energy Mater. 3 (2020) 705–714.
[106] Q.Z. Zhang, M.H. Zhou, G.B. Ren, et al., Nat. Commun. 11 (2020) 1731.
[107] X.C. Liu, W.Q. Li, Y.R. Wang, et al., Environ. Sci. Technol. 53 (2019) 6927–6936.
[108] S.O. Ganiyu, M. Zhou, C.A. Martínez-Huitle, Appl. Catal. B: Environ. 235 (2018) 103–129.
[109] X. Liu, Y. Zhou, J. Zhang, et al., Chem. Eng. J. 347 (2018) 379–397.
[110] Z. Wang, M. Liu, F. Xiao, et al., Chin. Chem. Lett. 33 (2022) 653–662.
[111] C.M. Sánchez-Sánchez, E. Expósito, J. Casado, V. Montiel, Electrochem. Commun. 9 (2007) 19–24.
[112] I. Ouiriemmi, A. Karrab, N. Oturan, et al., J. Electroanal. Chem. 797 (2017) 69–77.
[113] M. Luo, S. Yuan, M. Tong, et al., Water Res. 48 (2014) 190–199.
[114] Z.H. Wen, S.Q. Ci, F. Zhang, et al., Adv. Mater. 24 (2012) 1399–1404.
[115] X. Du, S. Wang, F. Ye, Z. Qingrui, Environ. Res. (2021) 112414.
[116] X. Du, W. Fu, P. Su, J. Cai, M. Zhou, Chem. Eng. J. 398 (2020) 125681.
[117] P. Hu, M. Long, Appl. Catal. B: Environ. 181 (2016) 103–117.
[118] L. Duan, N. Jiang, N. Lu, et al., Appl. Catal. B: Environ. 221 (2018) 521–529.
[119] L.L. Zhu, J.H. Ji, J. Liu, et al., Angew. Chem. Int. Ed. 59 (2020) 13968–13976.
[120] M. Wang, G. Fang, P. Liu, et al., Appl. Catal. B 188 (2016) 113–122.
[121] Y. Tian, M. Zhou, Y. Pan, X. Du, Q. Wang, Chem. Eng. J. 403 (2021) 126361.
[122] H. Zhao, Y. Wang, Y. Wang, T. Cao, G. Zhao, Appl. Catal. B: Environ. 125 (2012) 120–127.
[123] Y. Zhang, M. Gao, S.G. Wang, et al., Electrochim. Acta 231 (2017) 694–704.
[124] P. Su, M. Zhou, G. Ren, et al., J. Mater. Chem. A 7 (2019) 24408–24419.
[125] M. Sun, X.R. Ru, L.F. Zhai, Appl. Catal. B: Environ. 165 (2015) 103–110.
[126] H. Zhao, L. Qian, Y. Chen, Q. Wang, G. Zhao, Chem. Eng. J. 332 (2018) 486–498.
[127] X. Zhou, D. Xu, Y. Chen, Y. Hu, Chem. Eng. J. 384 (2020) 123324.
[128] T. Luo, H. Feng, L. Tang, et al., Chem. Eng. J. 382 (2020) 122970.
[129] L. Cui, Z. Li, Q. Li, et al., Chem. Eng. J. 420 (2021) 127666.
[130] X.C. Liu, W.Q. Li, Y.R. Wang, et al., Environ. Sci. Technol. 53 (2019) 6927–6936.
[131] D. Seibert, F. Henrique Borba, F. Bueno, et al., Chem. Eng. J. 372 (2019) 471–482.
[132] M.N. Chong, B. Jin, C.W.K. Chow, C. Saint, Water Res. 44 (2010) 2997–3027.
[133] X. Jia, L. Xie, Z. Li, et al., Sci. Total Environ. 768 (2021) 144368.
[134] L. Fu, S.J. You, G.Q. Zhang, F.L. Yang, X.H. Fang, Chem. Eng. J. 160 (2010) 164–169.
[135] M. Hassan, G.A. Ashraf, B. Zhang, et al., Chem. Eng. J. 380 (2020) 122483.
[136] C.H. Feng, F.B. Li, H.J. Mai, X.Z. Li, Environ. Sci. Technol. 44 (2010) 1875–1880.
[137] W. Yan, Y. Xiao, W. Yan, et al., Chem. Eng. J. 358 (2019) 1421–1437.
[138] P. Xu, D. Zheng, Z. Xie, et al., Sep. Purif. Technol. 234 (2020) 116103.
[139] Y.T. Wang, R.S. Wang, Materials 10 (2017) 169.
[140] M. Hassan, N. Pous, B. Xie, et al., Bioresour. Technol. 243 (2017) 949–956.
[141] Q. Wen, F. Kong, H. Zheng, et al., Chem. Eng. J. 168 (2011) 572–576.
[142] S. Long, L. Zhao, J. Chen, et al., Bioresour. Technol. 322 (2021) 124534.
[143] T. Hua, S. Li, F. Li, et al., Biochem. Eng. J. 146 (2019) 1–9.
[144] N. Li, Y. Wan, X. Wang, Sci. Total Environ. 706 (2020) 135690.
[145] M.N. Young, N. Chowdhury, E. Garver, et al., J. Power Sources 356 (2017) 448–458.
[146] J. Sim, R. Reid, A. Hussain, J. An, H.S. Lee, Biotechnol. Rep. 19 (2018) e00276.
[147] H. Dong, X. Liu, T. Xu, et al., Bioresour. Technol. 247 (2018) 684–689.
[148] M. Hassan, H. Olvera-Vargas, X. Zhu, B. Zhang, Y. He, J. Power Sources 424 (2019) 220–244.
[149] X.Q. Wang, C.P. Liu, Y. Yuan, F.B. Li, J. Hazard. Mater. 275 (2014) 200–209.
[150] D. Pant, G. Van Bogaert, L. Diels, K. Vanbroekhoven, Bioresour. Technol. 101 (2010) 1533–1543.
[151] H.-I. Kim, O.S. Kwon, S. Kim, W. Choi, J.-H. Kim, Energy Environ. Sci. 9 (2016) 1063–1073.
[152] S. Zhao, X. Zhao, H. Zhang, J. Li, Y. Zhu, Nano Energy 35 (2017) 405–414.
[153] G.H. Moon, W. Kim, A.D. Bokare, N.E. Sung, W. Choi, Energy Environ. Sci. 7 (2014) 4023–4028.
[154] L. Clarizia, D. Russo, I. Di Somma, R. Marotta, R. Andreozzi, Appl. Catal. B: Environ. 209 (2017) 358–371.
[155] D. Du, W. Shi, L. Wang, J. Zhang, Appl. Catal. B: Environ. 200 (2017) 484–492.
[156] L. Yang, G. Dong, D.L. Jacobs, et al., J. Catal. 352 (2017) 274–281.
[157] Z. Zhu, H. Pan, M. Murugananthan, J. Gong, Y. Zhang, Appl. Catal. B: Environ. 232 (2018) 19–25.
[158] Y. Shiraishi, S. Kanazawa, Y. Kofuji, et al., Angew. Chem. Int. Ed. 53 (2014) 13454–13459.
[159] S. Zhao, T. Guo, X. Li, et al., Appl. Catal. B: Environ. 224 (2018) 725–732.
[160] S. Hu, X. Qu, P. Li, et al., Chem. Eng. J. 334 (2018) 410–418.
[161] A. Torres-Pinto, M.J. Sampaio, J. Teixo, et al., J. Water Process. 37 (2020) 101467.
[162] X. Gao, C. Ma, Y. Liu, L. Xing, Y. Yan, Appl. Surf. Sci. 467-468 (2019) 673–683.
[163] U.M. García Pérez, S. Sepúlveda Guzmán, A. Martínezde la Cruz, U. Ortiz Méndez, J. Mol. Catal. A: Chem. 335 (2011) 169–175.
[164] T.L. Xia, Y.C. Lin, W.Z. Li, M.T. Ju, Chin. Chem. Lett. 32 (2021) 2975–2984.
[165] X. Wang, X. Zhang, Y. Zhang, et al., J. Mater. Chem. A 8 (2020) 15513–15546.
[166] Y. Xing, X. Wang, S. Hao, et al., Chin. Chem. Lett. 32 (2021) 13–20.
[167] S. Zhang, H. Gao, Y. Huang, et al., Environ. Sci. Nano 5 (2018) 1179–1190.
[168] P. Karaolia, I. Michael-Kordatou, E. Hapeshi, et al., Appl. Catal. B: Environ. 224 (2018) 810–824.
[169] Z. Xiong, L.L. Zhang, X.S. Zhao, Chem 17 (2011) 2428–2434.
[170] H. Zhang, W. Yang, J. Deng, J. Polym. Sci. Part A: Polym. Chem. 53 (2015) 1816–1823.
[171] A. Fleming, Bull. WHO 79 (2001) 780–790.
[172] D. Zhi, J. Wang, Y. Zhou, et al., Chem. Eng. J. 383 (2020) 123149.
[173] A. Cuprys, P. Thomson, Y. Ouarda, et al., J. Hazard. Mater. 389 (2020) 121890.
[174] A. Aboudalle, H. Djelal, F. Fourcade, et al., J. Hazard. Mater. 359 (2018) 85–95.
[175] J. Vidal, C. Huiliñir, R. Santander, et al., Sci. Total Environ. 624 (2018) 1095–1105.
[176] A.R. Rahmani, D. Nematollahi, M.R. Samarghandi, M.T. Samadi, G. Azarian, J. Electroanal. Chem. 808 (2018) 82–89.
[177] B.M.B. Ensano, L. Borea, V. Naddeo, M.D.G. de Luna, V. Belgiorno, Environ. Sci. Pollut. Res. 26 (2019) 1103–1112.
[178] X. Song, D. Huang, L. Zhang, et al., Electrochim. Acta 330 (2020) 135187.
[179] W.L. Jiang, X. Xia, J.L. Han, et al., Environ. Sci. Technol. 52 (2018) 9972–9982.
[180] D. Guo, Y. Liu, H. Ji, et al., Environ. Sci. Technol. 55 (2021) 4045–4053.